PAPER • **OPEN ACCESS**

Influence of link spacing on concrete shear capacity: experimental investigations and finite element studies

To cite this article: W Don *et al* 2020 *IOP Conf. Ser.: Mater. Sci. Eng.* **930** 012052

Influence of link spacing on concrete shear capacity: experimental investigations and finite element studies

W Don[1], K Chong[1], M Aitken[1], A Tambusay[1,2], B Suryanto[1]* and P Suprobo[2]

[1] Institute for Infrastructure and Environment, School of Energy, Geoscience, Infrastructure and Society, Heriot-Watt University, Edinburgh, United Kingdom.
[2] Department of Civil Engineering, Faculty of Civil, Planning and Geo Engineering, Sepuluh Nopember Institute of Technology, Surabaya, East Java, Indonesia.

*Corresponding author's e-mail: B.Suryanto@hw.ac.uk

Abstract. This paper investigates the influence of varying the spacing of shear reinforcement on the response of six geometrically identical reinforced concrete beams. Each beam was designed with differing longitudinal and transverse reinforcement configurations to provide improved understanding of the importance of providing sufficient shear reinforcement following guidance provided in Eurocode 2. Three different cases of varying transverse reinforcements were tested: one without the presence of shear reinforcement, one with shear reinforcement non-compliant to the design provisions and one where the design of the beams fully complies with the design guidance. In order to verify the experimental results, an open source digital image correlation software was utilised to allow for a computational crack mapping, along with the use of nonlinear finite element analysis software to enable a more thorough investigation of the individual beam response. The results obtained highlighted that shear links non-compliant to Eurocode 2 consequently led to unpredictable modes of failure, whereas beams containing shear links at the required amount and spacings displayed significant improvements in the mode of failure and ductility. Beams with the omittance of shear links resulted in the lowest load capacity, due to the sudden, brittle shear failure.

1. Introduction

Concrete is a highly versatile material that possesses high compressive strength but low tensile resistance. When combined with steel reinforcement, however, concrete can provide the ability to withstand significant tensile loads and exhibit excellent ductility, allowing structural elements to fail in a ductile manner with extensive plastic deformation when overloaded. This type of failure is commonly referred to as the flexural failure and is the desired failure mechanism. This mode of failure is generally aimed for in the design of a structural element due to the ability to provide ample warning before failure ultimately takes place. This behavioural response can be predicted to a high degree of accuracy with the utilisation of the current design specifications. Furthermore, the margin of safety of reinforced concrete members can be increased by designing members that are under reinforced in flexure which enables a gradual structural failure to occur.

To avoid a sudden catastrophic shear failure, shear reinforcement are generally provided with the main purpose of increasing the shear capacity of the structural concrete [1]. By increasing the spacing between the shear links, the potential can arise for inclined shear cracks to propagate between the links. In practice, this can be found in structural beam design subjected to relatively low shear stresses

commonly utilised in regions with none-to-low seismic activity and in a lightly reinforced, deep transfer beam [2]. In many cases of the design of reinforced concrete elements, where the concrete alone provides enough shear resistance against the low shear stresses imposed, it is good practice to provide minimum shear reinforcement. It is essential that the degree of safety of the elements is analysed and preventive measures are imposed to mitigate any potential catastrophic damage to occupants and society. Hence provisions of maximum spacing are given in current design codes to ensure the presence of at least one shear link in any potential formation of a diagonal shear crack. Furthermore, to ensure that the stirrups are adequately anchored in the concrete (hence effective to prevent a premature shear failure), Eurocode 2 [4], for example, limits the spacing of shear links in the longitudinal axis to be no more than the lesser of 0.75d or 600 mm. Other design codes specify more conservative limits; for example, ACI 318-14 [5] limits the longitudinal spacing to the lesser of 0.5d or 600 mm (or the lesser of 0.25d or 300 mm in members subjected to significant shear stress); JSCE [6] to the lesser of 0.5d or 300 mm in areas requiring shear link and the lesser of 0.75d or 400 mm in other areas; and CSA A23.3-04 [7] to the lesser of 0.63d or 600 mm. This design aspect is obviously very simple to implement yet essential, as if this is overlooked or ignored can potentially lead to a brittle, undesirable shear failure.

The paper provides an analysis of the behaviour of six steel reinforced concrete beams designed with varying tensile reinforcement ratios and varying shear reinforcement spacing. Two beams are designed in accordance with the current design provisions in Eurocode 2, with the remainder of the four beams designed with none to non-complying shear reinforcements. A principal focus in the paper is the effect of the variation of the spacing of the shear links on the overall structural response covering different design aspects from standard to non-complicit design. To this end, digital image correlation (DIC) [8-11] is utilised to allow for a detailed crack development during the experimental testing of the beams to be monitored and verify the experimental behaviour during testing. Alongside this, nonlinear finite element analysis (FEA) is also undertaken to study the underlying mechanisms exhibited by each beam, using the ATENA Science software package [12]. In this paper, it is shown that through the use of these advanced modern-day computational methods (FEA and DIC), more refined understanding of the shear behaviour can be obtained which will increase the understanding of the significance of the shear spacing in the shear design of reinforced concrete members.

2. Experimental Programme

The experimental programme involved the testing of six geometrically identical reinforced concrete beams under four-point loading. All beams had a 150×250 mm rectangular cross-section dimension and a 30mm clear concrete cover to the main bars. The only varying parameter between specimens were the longitudinal and transverse (shear) reinforcement arrangements. The geometry and breakdown of all the reinforcement layouts of the specimens are illustrated in figure 1. The first three beams were reinforced with three H12 bottom bars (denoted L series), whereas the remaining three beams had two H16 bottom bars (denoted H series)– corresponding to longitudinal reinforcement ratios of 1.06% and 1.26%, respectively. Two of the beams in each series had H8 transverse reinforcement provided at a spacing of 300 mm (≈1.4d) and 150 mm (≈0.7d) over the shear span, corresponding to the shear reinforcement ratios of 0.22% and 0.45%, respectively. No transverse and longitudinal top reinforcements were provided in the remaining two beams (Beams L1 and H1).

2.1. Materials, fabrication and curing

Casting of the test specimens occurred on two separate days, using the same grade of concrete (C25/30) and slump (S2). The concrete was ordered from a local ready-mix company, with each batch used to fabricate three beams. Table 1 provides a breakdown of the mix design for the concrete, together with the corresponding concrete compressive strength for each beam. The concrete strengths were computed from the conversion of the mean strengths of three concrete cube samples with dimensions of 100×100×100 mm at the day of testing. All beams were cured under a wet burlap, wrapped in polyethylene sheeting at ambient laboratory conditions until approximately three days prior to testing. All beams were tested between 23 and 30 days after casting.

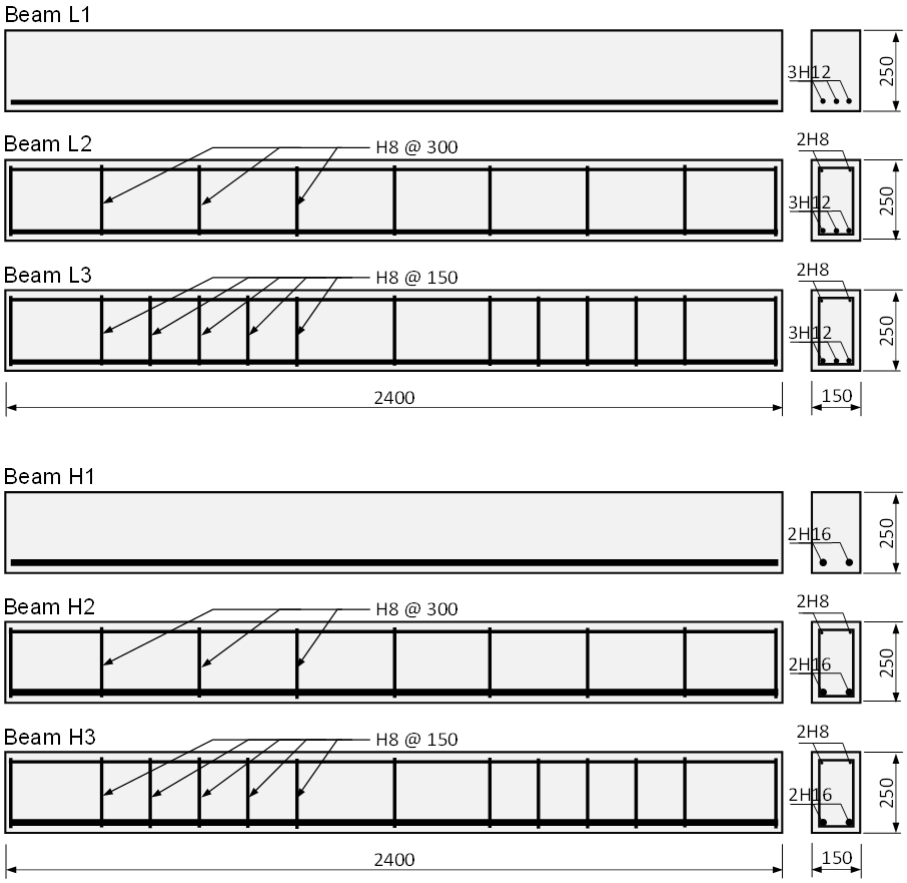

Figure 1. Beam geometry and bar configuration (dimension in mm). In each beam, 30 mm clear cover was provided to the main bars.

Table 1. Summary of concrete mix and strengths. (WRA: BASF Glenium 126).

OPC (kg/m^3)	GGBS (kg/m^3)	4/20 mm (kg/m^3)	0/4 mm (kg/m^3)	WRA (kg/m^3)	w/b	Compressive strength (MPa)					
						L1	L2	L3	H1	H2	H3
150	150	1020	940	1.7	0.6	23.8	25.8	26.5	29.8	31.1	31.6

2.2. Test configurations and measurement

The schematic of the test setup is presented in figure 2. Prior to testing, each beam was simply supported on two solid steel rods placed 1800mm apart, with the support configuration of a pin at one end (by means of a steel rod welded to a pair of steel plates) and a roller at the other end (by means of a steel rod free to rotate between two steel plates). The equipment used to perform the monotonic loading was a 2000kN Losenhausen servo-hydraulic testing machine. The load was applied through a rigid spreader (steel) beam to direct the load from the testing rig to two 50 mm diameter steel rods placed 600mm apart. At all loading and support points, steel plates with dimensions of 100×60×200 mm were provided. The loading imposed on the test beams under a crosshead speed of 0.5mm/min, paused at regular intervals of 10kN to allow for the manual crack mapping of the beam to progress. The imposed loads were recorded using a load cell installed in the test rig, while the beam deflections were recorded using one LVDT (linear variable displacement transducer) placed under the beam at the midspan. All data was recorded using a 16-bit USB data acquisition system at a sampling rate of 5Hz.

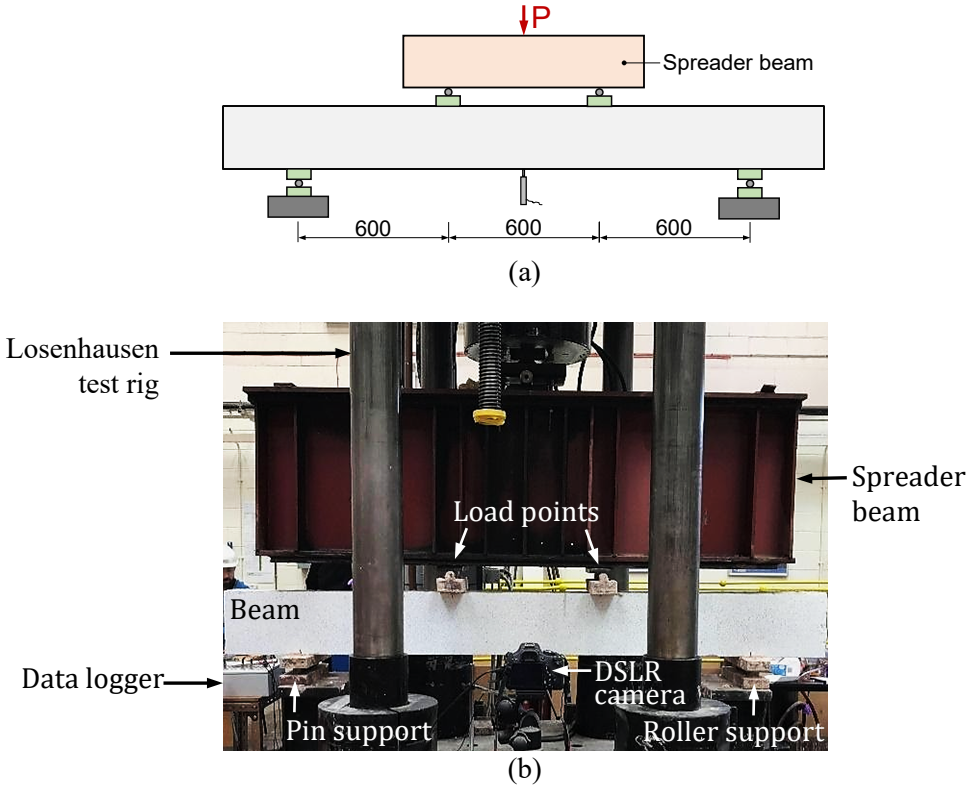

Figure 2. (a) Schematic of test setup; (b) typical view prior to testing.

Prior to testing, the both sides of each beam were whitewashed. Grid lines were then drawn on one side to allow for the manual crack mapping during the testing process. The other side was sprayed with a random black speckle pattern to facilitate the digital crack mapping. This was done by recording the crack development on the beam surface at 2kN increments using a 18MP Canon EOS Rebel T3i digital camera. The acquired digital images were then analysed using an open-source DIC software Ncorr to obtain crack development and failure mode [8-11]. The camera was mounted on a sturdy tripod and controlled remotely through a Desktop PC to avoid inadvertent camera movement throughout the testing process.

3. Nonlinear Finite Element Analysis

Three-dimensional nonlinear finite element analyses were undertaken for each beam using ATENA Science software package, developed by Červenka Consulting [12]. Figure 3(a) displays the typical finite element meshes used to represent the beams. The concrete was modelled using 8-node hexahedral elements with a typical size of 30 mm. The embedded reinforcement was modelled using a one-dimensional element. The plates at the loading and support points were modelled using an elastic tetrahedral element. In this study, the "Cementitious2 User" model was used for the concrete.

Figures 3(b) and (c) display a summary of the compression, tension and shear transfer models implemented in the software package. In the compression model, the compression hardening function is defined using an elliptical relation through the following expression [12,13]

$$\frac{\sigma_c}{f_c'} = f_{co} + (f_c' - f_{co})\sqrt{1 - \left(\frac{\varepsilon_c - \varepsilon_c^p}{\varepsilon_c}\right)^2} \quad (1)$$

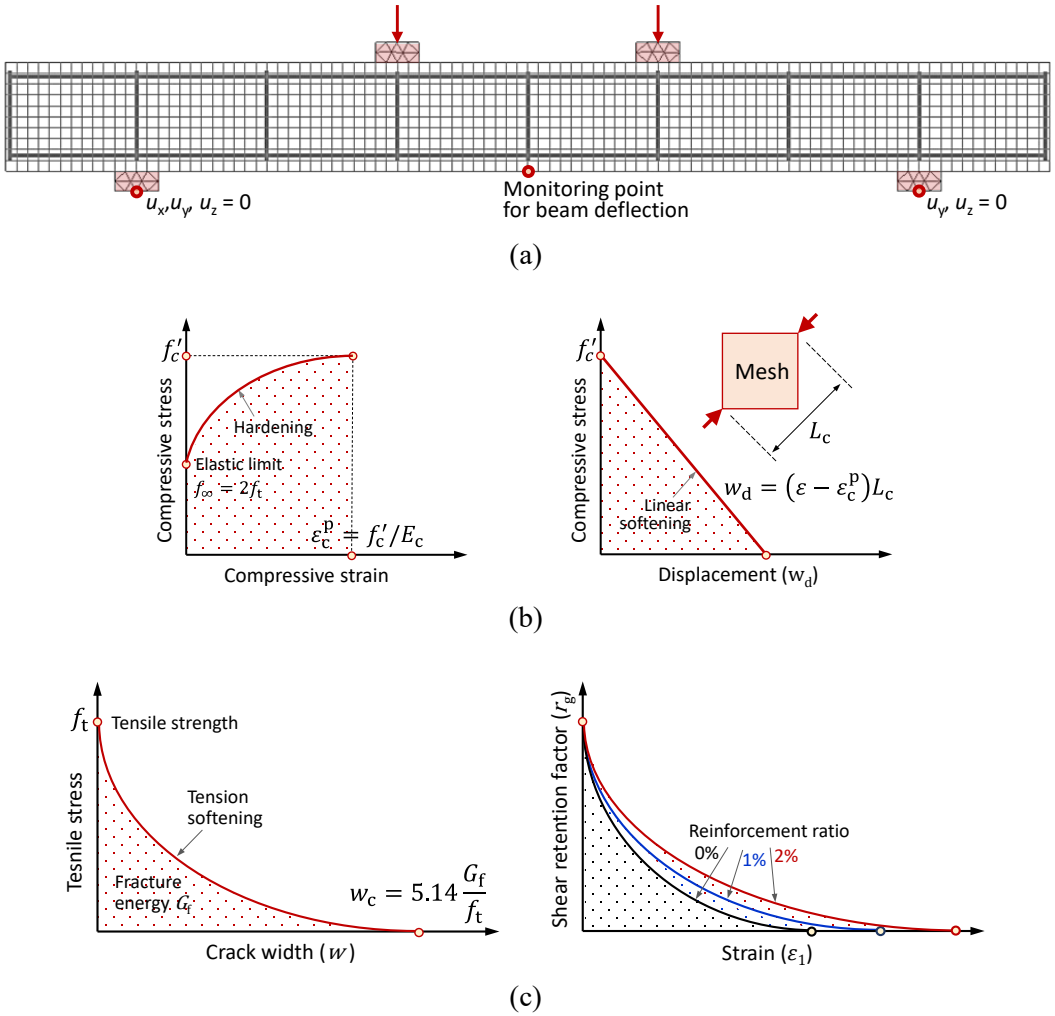

Figure 3. (a) Typical finite element mesh; (b) compression model; and (c) tension and shear transfer models.

where σ_c is the normal compressive stress (MPa); f'_c is the mean cylinder compressive strength (MPa); f_{co} is the compressive stress at post-elastic point (MPa); ε_c is the concrete strain (mm/mm); and ε_c^p is the plastic strain at the peak point (mm/mm). Beyond the peak, the softening relation is determined through an analogical model commonly known as the crush band model (to ensure mesh objectivity) [14]. The assumption was made on the localisation of post-peak compressive stress and energy dissipation in a plane normal to the direction of principal stress. A w_d value of 0.05 mm was used in this study following the recommended value for normal concrete [15].

In the tension model, the exponential softening law is adopted following the formulation of fictitious crack model based on the crack-opening law and fracture energy which are expressed in the following manner [12],

$$\frac{\sigma_t}{f_t} = \left(1 + \left(c_1 \frac{w}{w_c}\right)^3\right) \exp\left(-c_2 \frac{w}{w_c}\right) - \frac{w}{w_c}(1 + {c_1}^3)\exp(-c_2) \quad (2)$$

where σ_t is the normal tensile stress (MPa); f_t is the tensile cracking strength (MPa); w is the crack opening (mm); and w_c is the crack opening at the complete release of stress deriving from fracture energy (mm). Empirical constants $c_1 = 3$ and $c_2 = 6.93$ are considered.

The shear transfer model of cracked concrete is represented by a shear retention factor following the formulation proposed by Kolmar [16]. The shear modulus is related to the strain normal to the crack which is indicative of crack opening. For more detailed information of cementitious user material used in this study, readers are referred to reference [12].

4. Results and Discussion

4.1. Test observations

Figures 4(a) and (b) present the load applied at one side of each beam plotted against the mid-span deflection for L and H series beams respectively. For illustrative purposes, figure 5 displays typical failure crack patterns obtained from the L series beams (comparable crack patterns were obtained from the H series beams). During testing, flexural cracking was first observed at a shear (half of the machine) load of approximately 8kN, which corresponds to a moment value of 4.8kNm and tensile stress in the concrete at the bottom most part of the beam of approximately 3.1MPa. At increasing loads, new flexural cracks formed along the length of the beam, while pre-existing cracks extended vertically and increased in width. As displayed in figures 4(a) and (b), this resulted in a significant reduction in beam stiffness. It is interesting to note that the post-cracking response of the beams in each series was similar to each other and once the cracks had uniformly developed, the response followed an approximately straight line at a slope of approximately 30% of the initial (pre-cracking) stiffness. However, this trend is only true up to the formation of significant diagonal shear cracks, which occurred (initially) at one (weaker)

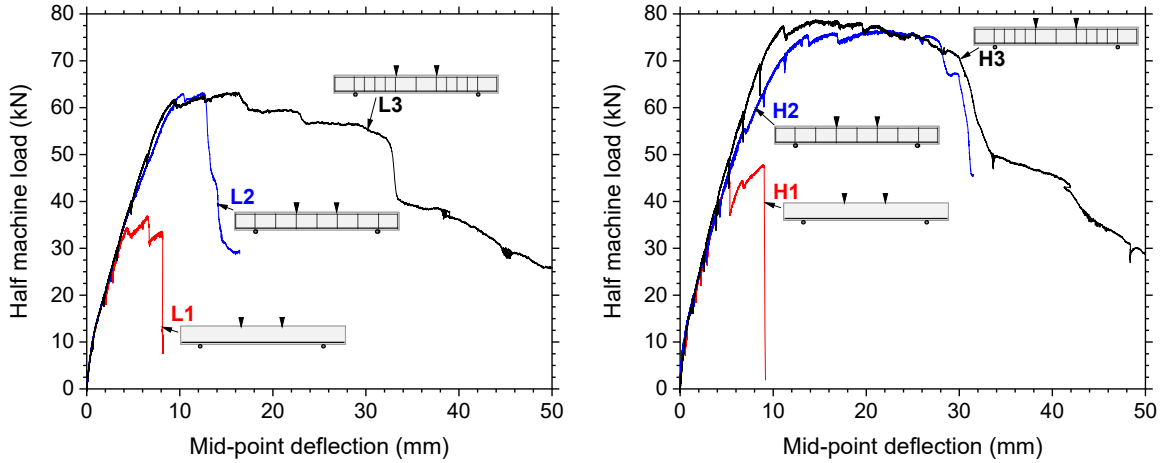

Figure 4. Shear-deflection response: (a) Beams L1–3 and (b) Beams H1–3.

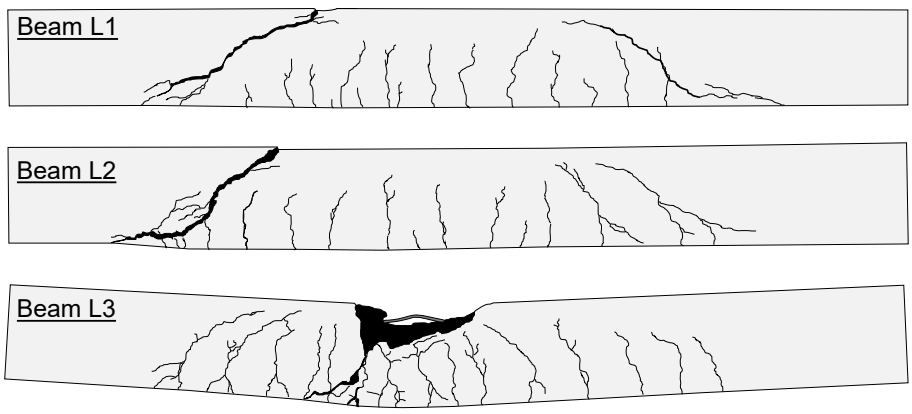

Figure 5. Typical crack patterns after failure.

side of a beam, at an applied shear load of ~35kN for Beam L1 and ~45kN for Beam H1. Failure finally occurred when the diagonal shear crack had extended to the point of load application and propagated down to the support along the top of the bottom reinforcement, leading to the formation of an *S-shaped* failure crack pattern. The failure was brittle, as indicated by the sudden drop in load-carrying capacity.

As the spacing of the transverse reinforcement is decreased from 600 mm (Beams L1 and H1) to 150 mm (Beams L3 and H3), the mode of failure is altered from shear to flexure. This is attributed to the fact that in these beams, the failure load that corresponds to the shear capacity is higher than that of the flexural capacity. It is interesting to note that although this relation also applies to Beams L2 and H2, these beams failed in shear as the spacing of transverse links in these two beams did not satisfy the maximum link spacing outlined in Eurocode 2 (0.75d or, in this case ~160 mm). Shear crack can, therefore, develop between two shear links where the shear is resisted only by the concrete. The evidence for this can be seen from figure 5 in which the formation of the diagonal (shear) crack between two shear links is clearly evident, with the crack at the mid-depth forming at an angle of ~70^{o} from the horizontal (or an increase of ~25^{o} from the angle of the critical crack in Beam L1).

With reference to figures 4(a) and (b), it is interesting to note that although Beams L2 and H2 could not develop to their full load capacity (based on the amount of the shear links provided), the shear capacities of these beams exceeded the shear capacity of the concrete itself by a considerable amount (compare, for example, the load capacity of Beams L2 and H2 to Beams B1 and L1). This could be related to the general increase in shear strength with an increase in shear span-to-depth (a/d) ratio [17] (with the increase in this ratio is dictated by the spacing of the shear reinforcement), although the presence of the transverse links might have also prevented the propagation of the critical shear crack and hence makes a contribution to the overall increase in shear capacity. At this moment, however, it is not possible to obtain a quantitative measure of the increase in shear capacity as the tension bars in both beams reached their yield capacity before the beam reached the shear capacity. It is also still not clear as to why Beam H2 was able to continue to resist considerable load after the formation of a diagonal crack at a shear load of approximately 56kN (see the slight drop in load in figure 4(b)). This is possibly due to the presence of the shear links as stated above; however, further investigation is needed to clarify this issue.

4.2. Crack developments

To provide detailed insights into the response of the beams, figure 6 illustratively displays the formation and propagation of concrete cracks in Beams L1 and L2 obtained from the DIC crack mapping.

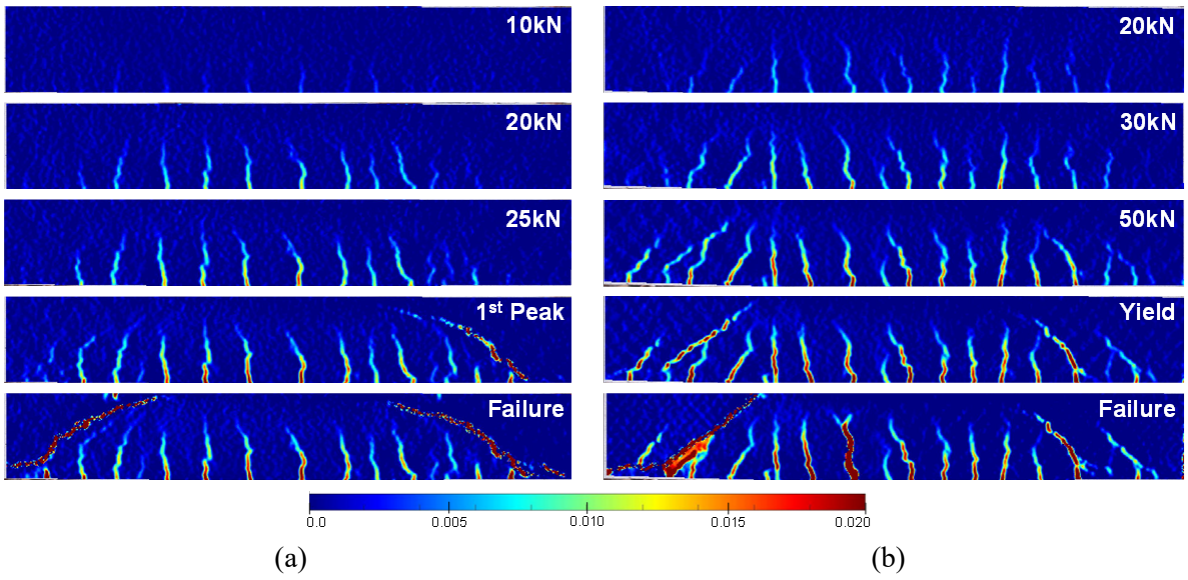

Figure 6. Crack developments at selected load levels during testing: (a) Beam L1 and (b) Beam L2.

It is evident from figure 6 that at early stages of loading, both beams exhibited uniform crack distribution, consisting primarily of flexural cracks which extend vertically with increasing loads. Some of the cracks over the side (shear) span then developed a rotation at their tips and merged with other cracks to develop a critical crack at both ends of the beam. This critical crack then propagated towards the point of load application at the top and down to the top layer of tension reinforcement and continued as a nearly horizontal (splitting) crack along the tension steel. This resulted in a sudden and brittle failure, with no ductility beyond the peak load (see figures 4(a) and (b)).

4.3. Nonlinear finite element analysis

The load (applied at one side of each beam) vs midspan deflection responses for all beams obtained from the finite element analyses are presented in figures 7(a) and (b), and can be compared to experimental results presented earlier in figures 4(a) and (b). As can be seen, there is an excellent agreement between the predicted and observed responses in terms of the overall load-deflection response and mode of failure. It is evident that as the spacing of transverse reinforcement decreases, the load capacity and ductility of the beams increase; this behaviourial response could be well captured by the simulations. The predicted and observed failure crack patterns are also in good agreement (compare, for example, figures 5 and 7). Of interest to note is the successful representation of the increasing angle of the failure crack in beams with intermediate link spacing (i.e. Beams L2 and H2). The crack patterns over the centre span could also be well simulated and are similar to the experimental crack patterns displayed previously in figure 6, highlighting the value and and accuracy of the finite element models employed in this study.

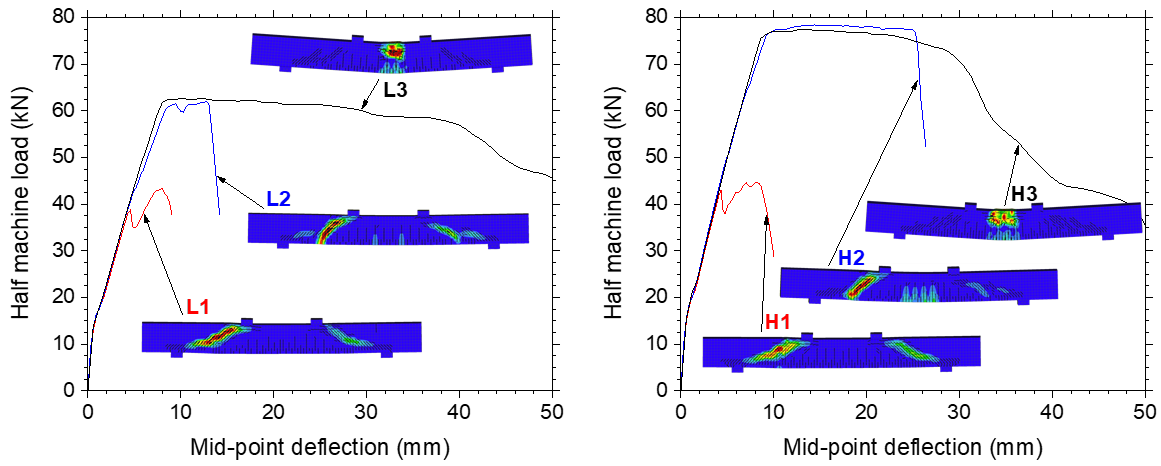

Figure 7. Predicted shear-deflection response for (a) Beams L1–3 and (b) Beams H1–3.

5. Concluding remarks and conclusions

Six geometrically identical beams produced from two batches to the same specification of concrete mix (C25/30) were tested. Beams L1 and H1 had no shear reinforcement; Beams L2 and H2 were non-compliant with the necessary shear reinforcement spacing detailed in Eurocode 2 and Beams L3 and H3 fully complied with this provision. The purpose of this study was to determine the influence of varying the link spacing on the shear capacity of each concrete section. This was achieved by performing experimental testing, digital crack mapping and nonlinear finite element analyses. The following conclusions can be drawn:

1. Beams L1 and H1 yielded the lowest load bearing capacities. With the omittance of shear reinforcement, the beams, as expectedly, failed in shear at a maximum load of 35kN and 45kN while exhibiting very low ductility. These beams are crucial in highlighting the dangerous, sudden brittle failure which can occur in structural members with no shear reinforcement.

2. Beams L2 and H2 exhibited significantly higher load bearing capacities and deflections than those discussed previously. However, the subsequent differing modes of failure highlights how inadequate spacing of shear links can lead to unpredictable responses. Shear failure occurred regardless of the inclusion of shear linkages due to the lack of sufficient spacing.
3. Beams L3 and H3 yielded load bearing capacities similar to that of L2 and H2 respectively. However, of major significance is the change from shear to flexural failure. As a result of the sufficient spacing of shear links, the brittle premature shear failure could be prevented. Instead, the mode of failure was very ductile, with the gradual propagation of cracks and the beam deflecting significantly more than the previous designs. This behaviour is sought after by structural designers as it allows adequate warning before failure ultimately occurs.
4. Nonlinear finite element analyses show strong agreements on the overall load-deflections and failure modes of the beams tested, validating the experimental behaviours exhibited. Moreover, the use of digital image correlation further exacerbated the accuracy between analyses and testing through detailed crack mapping throughout the testing.
5. It is shown that errors in the design of a structural member can potentially be catastrophic and the use of advanced analysis tools could be useful in this regard; for example, for identifying potential problems or assessing behavioural response influencing the performance and safety of a structure.

References

[1] Suryanto B, Morgan R and Han A L 2016 Predicting the response of shear-critical reinforced concrete beams using Response-2000 and SNI 2847:2013 *Civ. Eng. Dimens.* **18** 1 16–24
[2] Collins M P and Kuchma D 1999 How safe are our large, lightly RC beams, slabs, and footings? *ACI Struc. J.* **96** 4 482–90
[3] Anderson B G 1957 Rigid frame failures *ACI J. Proc.* **53** 1 625–36
[4] BSI, 2015 *BS EN 1992-1-1:2004+A1:2014: Eurocode 2: Design of concrete structures. General rules and rules for buildings* London, British Standards Institution
[5] ACI, 2014 *ACI 318M-14 Building code requirements for structural concrete and commentary* Farmington Hills, American Concrete Institute
[6] JSCE, 2007 *Standard specifications for concrete structures – 2007 design* Tokyo, Japan Society of Civil Engineers
[7] CSA, 2019 *CSA A23.3:19 Design of concrete structures* Toronto, Canadian Standards Association
[8] Blaber J, Adair B and Antoniou A 2015 Ncorr: open-source 2D digital image correlation Matlab software *Exp. Mech.* **55** 6 1105–22
[9] Suryanto B, Tambusay A and Suprobo P 2017 Crack mapping on shear-critical reinforced concrete beams using an open source digital image correlation software *Civ. Eng. Dimens.* **19** 2 93–8
[10] Tambusay A, Suryanto B and Suprobo P 2018 Visualization of shear cracks in a reinforced concrete beam using the digital image correlation *Intr. J. Adv. Sci. Eng. Inf. Tech.* **8** 1 573–8
[11] Tambusay A, Suryanto B and Suprobo P 2020 Digital image correlation for cement-based materials and structural concrete testing *Civ. Eng. Dimens.* **22** 1 6–12
[12] Červenka V, Jendele L and Červenka J 2018 Program documentation ATENA theory Czech Republic, Červenka Consulting
[13] Menétrey P and Willam K J 1995 Triaxial failure criterion for concrete and its generalization *ACI Struc. J.* **95** 3 311–8
[14] Mier J G M V 1986 Multiaxial strain-softening of concrete part 1: fracture *Mat. Strut.* **19** 111 190–200
[15] Červenka J, Červenka V and Laserna S 2018 On crack band model in finite element analysis of concrete fracture in engineering practice *Eng. Fract. Mech.* **197** 27–47
[16] Kolmar W 1986 Specification of shear transfer across cracks in nonlinear finite element analysis of reinforced concrete structures *PhD Thesis* Darmstadt University of Technology Germany
[17] Collins M P, Bentz E C and Sherwood E G 2008 Where is shear reinforcement required? review of research results and design procedures *ACI Struc. J.* **105** 5 590–600